

Available online at [www.sciencedirect.com](http://www.sciencedirect.com)

ScienceDirect

[www.elsevier.com/locate/jes](http://www.elsevier.com/locate/jes)

**JES**  
 JOURNAL OF  
 ENVIRONMENTAL  
 SCIENCES  
[www.jesc.ac.cn](http://www.jesc.ac.cn)

# Advanced treatment of wet-spun acrylic fiber manufacturing wastewater using three-dimensional electrochemical oxidation

Tianlong Zheng<sup>1</sup>, Qunhui Wang<sup>1,2,\*</sup>, Zhining Shi<sup>3</sup>, Yue Fang<sup>1</sup>, Shanshan Shi<sup>1</sup>, Juan Wang<sup>1</sup>, Chuanfu Wu<sup>1</sup>

1. Department of Environmental Engineering, University of Science and Technology Beijing, Beijing 100083, China. E-mail: skytal\_03@sina.com  
 2. Beijing Key Laboratory on Resource-oriented Treatment of Industrial Pollutants, University of Science and Technology Beijing, Beijing 100083, China  
 3. School of Earth and Environmental Sciences, The University of Adelaide, South Australia 5005, Australia

## ARTICLE INFO

### Article history:

Received 22 January 2016

Revised 3 March 2016

Accepted 11 March 2016

Available online 28 April 2016

### Keywords:

Advanced treatment

Synergistic effect

Three-dimensional electrochemical oxidation

Wet-spun acrylic fiber wastewater

## ABSTRACT

A three-dimensional electrochemical oxidation (3D-EC) reactor with introduction of activated carbon (AC) as particle micro-electrodes was applied for the advanced treatment of secondary wastewater effluent of a wet-spun acrylic fiber manufacturing plant. Under the optimized conditions (current density of 500 A/m<sup>2</sup>, circulation rate of 5 mL/min, AC dosage of 50 g, and chloride concentration of 1.0 g/L), the average removal efficiencies of chemical oxygen demand (COD<sub>cr</sub>), NH<sub>3</sub>-N, total organic carbon (TOC), and ultraviolet absorption at 254 nm (UV<sub>254</sub>) of the 3D-EC reactor were 64.5%, 60.8%, 46.4%, and 64.8%, respectively; while the corresponding effluent concentrations of COD<sub>cr</sub>, NH<sub>3</sub>-N, TOC, and UV<sub>254</sub> were 76.6, 20.1, and 42.5 mg/L, and 0.08 Abs/cm, respectively. The effluent concentration of COD<sub>cr</sub> was less than 100 mg/L, which showed that the treated wastewater satisfied the demand of the integrated wastewater discharge standard (GB 8978-1996). The 3D-EC process remarkably improved the treatment efficiencies with synergistic effects for COD<sub>cr</sub>, NH<sub>3</sub>-N, TOC, and UV<sub>254</sub> during the stable stage of 44.5%, 38.8%, 27.2%, and 10.9%, respectively, as compared with the sum of the efficiencies of a two-dimensional electrochemical oxidation (2D-EC) reactor and an AC adsorption process, which was ascribed to the numerous micro-electrodes of AC in the 3D-EC reactor. Gas chromatography mass spectrometry (GC-MS) analysis revealed that electrochemical treatment did not generate more toxic organics, and it was proved that the increase in acute biotoxicity was caused primarily by the production of free chlorine.

© 2016 The Research Center for Eco-Environmental Sciences, Chinese Academy of Sciences.

Published by Elsevier B.V.

## Introduction

The acrylic fiber manufacturing industry is dominant in Asia as a result of the large demand of the global market. China is the country that produces the largest amount of acrylic fiber, with a yield of nearly 0.7 tons of acrylic fiber every year (Zheng et al., 2015a). The wastewater from production of acrylic fiber

contains complex, highly toxic, and poor biodegradable compounds, such as organic nitriles, alkanes, and aromatic organic compounds (Zheng et al., 2015b). Millions of tons of wastewater are generated during the process, which is a concern because the effluent is resistant to degradation by conventional biological treatment technologies. Therefore, it is essential to search for efficient treatment methods to

\* Corresponding author. E-mail: wangqh59@sina.com (Qunhui Wang).

**Table 1 – Characteristics of the acrylic fiber wastewater.**

Parameters	COD <sub>cr</sub> (mg/L)	BOD <sub>5</sub> (mg/L)	NH <sub>3</sub> -N (mg/L)	TOC (mg/L)	UV <sub>254</sub> (Abs/cm)	BOD <sub>5</sub> /COD <sub>cr</sub>	pH
Range of values	203–240	18–30	44–63	60–103	0.18–0.26	0.09–0.13	7.0–8.4
Mean value ± S.D.	215.8 ± 10.3	24 ± 4	51.2 ± 4.8	79.3 ± 13.4	0.23 ± 0.02	0.11 ± 0.01	7.9 ± 0.4

S.D. is the abbreviation of standard deviation.

BOD<sub>5</sub>: biochemical oxygen demand after 5 days.

eliminate the pollution risks of discharging acrylic fiber wastewater into sewer systems.

Presently, treatment techniques for acrylic fiber wastewater include electro-coagulation (Gong et al., 2014), the electro-Fenton process (Sun et al., 2015a), microelectrolysis (Lai et al., 2012), a novel biological treatment with an upflow anaerobic sludge blanket (UASB) (Li et al., 2011, 2012), sequencing bioreactor (SBR) (Li et al., 2013), ANAMMOX process (An et al., 2013) and hybrid anoxic/oxic membrane bioreactor (A/O-MBR) (Tian et al., 2015). However, there is no fully mature technology that is able to achieve the desired removal efficiency to meet discharge standards. Thus, it is increasingly urgent to find efficient techniques to reduce the amounts of contaminants in the wastewater. Three-dimensional electrochemical oxidation (3D-EC) technology with introduction of particle electrodes leads to higher specific surface area and shorter distance of mass transfer. The technique has been widely used in refractory wastewater treatment, including dyeing wastewater (Wang et al., 2005), landfill leachate (Zhang et al., 2010), CI acid orange 7 containing wastewater (Xu et al., 2008), paper mill wastewater (Wang et al., 2007), and heavy oil refinery wastewater (Wei et al., 2010). It has been considered as an effective and promising method for wastewater treatment (Zhang et al., 2013). However, there are few studies on the treatment of acrylic fiber wastewater using the 3D-EC process.

In this study, a 3D-EC reactor, with activated carbon (AC) introduced as particle electrodes, was utilized for advanced treatment of the secondary effluent of wastewater from the acrylic fiber manufacturing industry. The reactor parameters, including current density, circulation rate, AC dosage, and chloride concentration, were optimized, and then the removal rates of the contaminants were investigated under the optimized treatment conditions. The synergistic effect of the 3D-EC reactor was also explored to interpret its enhancement of the degradation of organics. Moreover, the biodegradability and acute biotoxicity of the wastewater were assessed to evaluate the environmental risk and industrial feasibility of the 3D-EC system.

## 1. Experimental

### 1.1. Wastewater

The experimental wastewater was the secondary effluent of an acrylic fiber manufacturing plant in Northern China. The wastewater was stored at 4°C. Physical and chemical properties of the raw wastewater are shown in Table 1. The raw wastewater is characterized by complicated components, high toxicity, and low biodegradability.

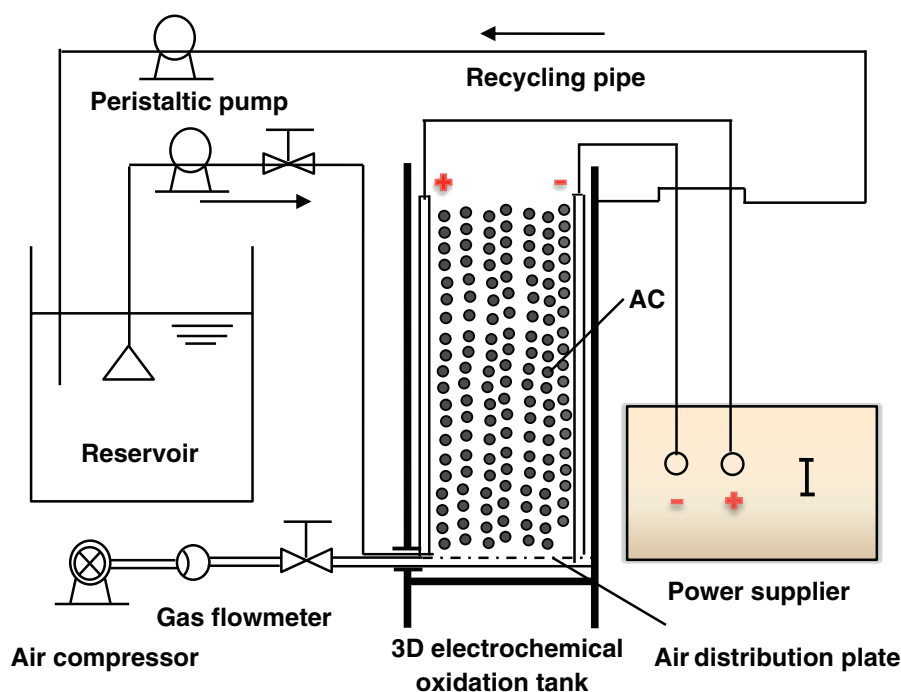


**Fig. 1 – Schematic diagram of the experimental setup.**

## 1.2. Experimental setup and procedure

The experimental setup is shown in Fig. 1. The apparatus consisted of a peristaltic pump, an air compressor, a power supply, a 3D-EC reactor, a pair of electrode plates, and a reservoir tank. The 3D-EC reactor was made of transparent rigid plexiglas with the dimensions of 20 mm (L) × 50 mm (W) × 70 mm (H), with working volume of 60 mL. A pair of titanium plates coated with RuO<sub>2</sub> and ZnO<sub>2</sub> was used as anode and cathode, respectively. The space between the two plates with a surface area of 30 cm<sup>2</sup> was 20 mm and was filled with granular activated carbon and ceramsite (volume ratio 1:1). The granular activated carbon consisted of particles of cylindrical shape with a diameter of 0.25 mm and length of 0.5 mm. Wastewater was fed and recycled in the 3D-EC reactor by a peristaltic pump. Based on the previous study (Anglada et al., 2009; Urtiaga et al., 2014; Fernandes et al., 2016), current densities from 120 to 700 A/m<sup>2</sup> were applied for the wastewater treatment system with a power supply, which supported electrochemical oxidation of wastewater among the anode, cathode, and AC particle micro-electrodes.

## 1.3. Analytical methods

Most of the wastewater quality parameters were measured according to The Water and Wastewater Monitoring and Analysis Method (4th edition) (Wei et al., 2002). In addition,

chemical oxygen demand (COD<sub>Cr</sub>), BOD<sub>5</sub>, total organic carbon (TOC), and ultraviolet absorption at 254 nm (UV<sub>254</sub>) were measured by a COD rapid digestion apparatus (DIS-1 A, Shenzhen Changhong Instru. Co., Ltd., China), OxiTop system (OxiTop, WTW, Germany), a Vario TOC analyzer (Vario TOC, Elementar, Germany) and a UV-visible spectrophotometer (UV-752, METASH, China), respectively. The toxicity of samples was analyzed using a Modulus Single Tube Luminometer (Turner Biosystems, USA), which is based on the light emission inhibition of luminescent bacteria, the methods of which can be found in Martins et al. (2010). Further, the toxicity level expressed as EC<sub>50</sub>, representing sample concentrations causing 50% bacteria inhibition, was acquired using serial dilutions of each sample. The pH of the reactor was monitored by an automatic potentiometric titrator meter (ZD-2, LEICI, China) at 20°C. Samples were filtered before measurement with a 0.45 μm PVDF membrane and were analyzed several times to validate the results.

## 1.4. Gas chromatography mass spectrometry (GC-MS) measurement

GC-MS was used for the analysis of the main organic compounds in the wastewater. In order to apply GC-MS analysis, 150 mL of the wastewater sample was extracted with 50 mL of CH<sub>2</sub>Cl<sub>2</sub> (Chromatogram Pure Grade, Fisher) three times under acidic (pH 2.0), neutral (pH 7.0), and

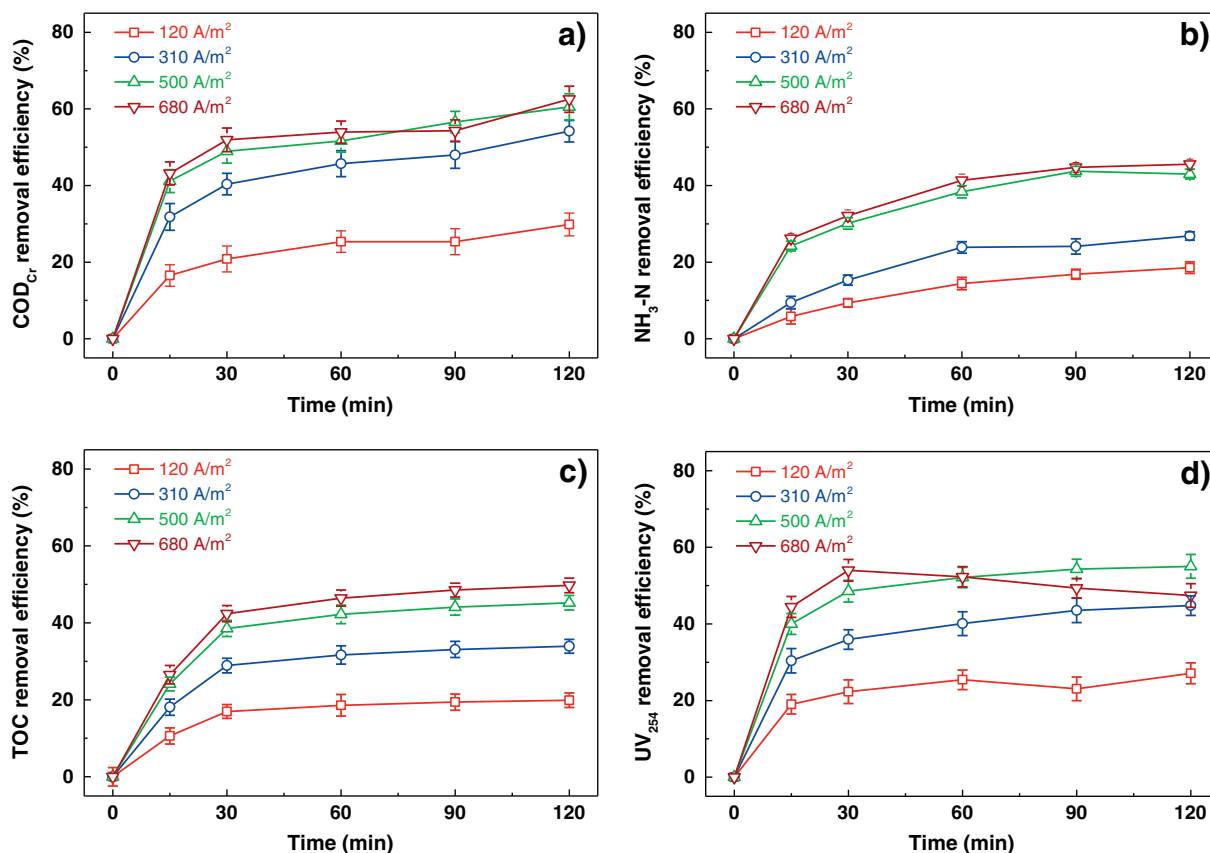


Fig. 2 – The effect of current density on the removal efficiencies of COD<sub>Cr</sub>, NH<sub>3</sub>-N, TOC, and UV<sub>254</sub> for the 3D-EC reactor. Error bars represent standard deviation of three replicates. COD<sub>Cr</sub>: chemical oxygen demand; TOC: total organic carbon; UV<sub>254</sub>: ultraviolet absorption at 254 nm; 3D-EC: three-dimensional electrochemical oxidation.

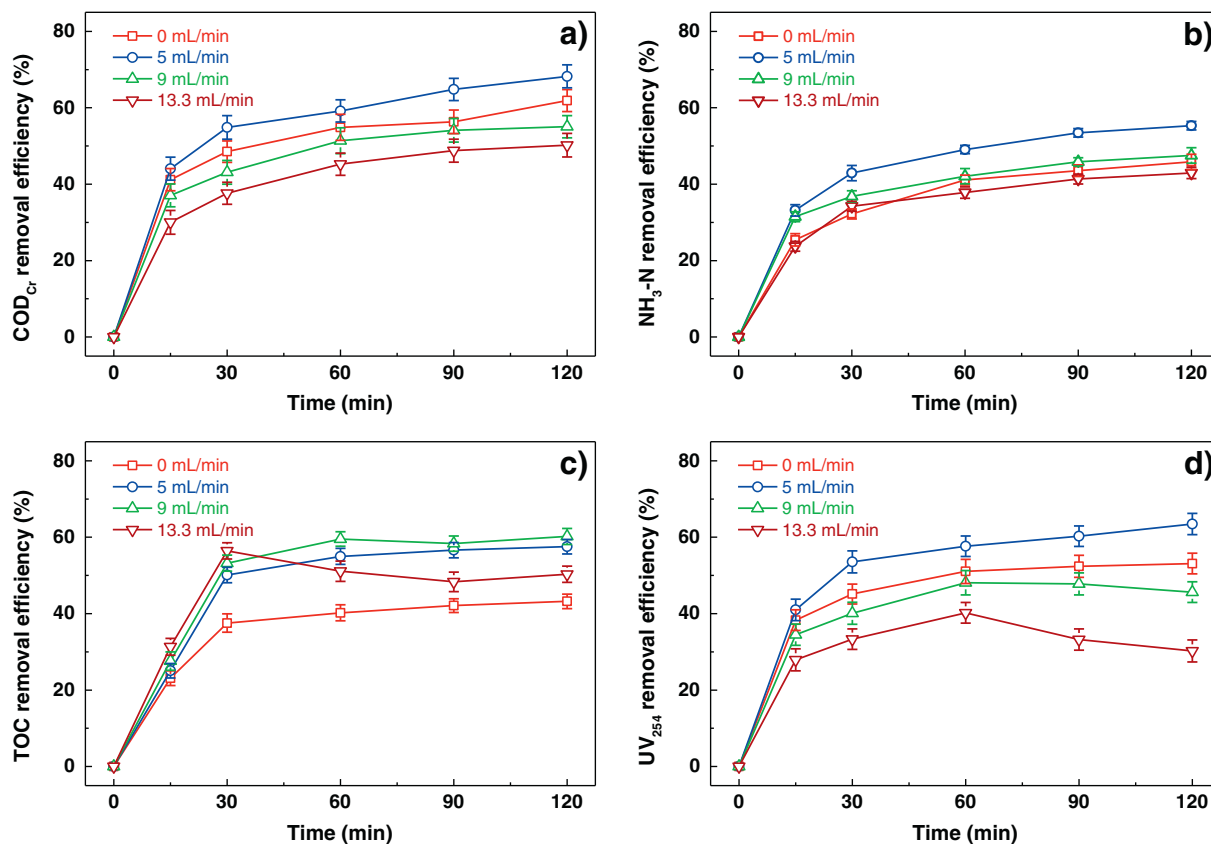


Fig. 3 – The effect of circulation rate on the removal efficiencies of  $\text{COD}_{\text{Cr}}$ ,  $\text{NH}_3\text{-N}$ , TOC, and  $\text{UV}_{254}$  for the 3D-EC reactor. Error bars represent standard deviation of three replicates.

alkaline (pH 12.0) conditions, respectively. The three extracts were mixed together, then the mixture was dehydrated with anhydrous sodium sulfate and dried under a flow of nitrogen gas. The residual was dissolved in 1.0 mL of  $\text{CH}_2\text{Cl}_2$  and then 1  $\mu\text{L}$  of the dissolved residual was injected into a Shimadzu GCMS-QP2010 plus system (Shimadzu, Japan). The column used in this system was a 30 m  $\times$  0.25 mm inner diameter (i.d.), J&W Scientific 122-5032 DB-5 (5% diphenyl-dimethylpolysiloxane; USA) capillary column with a film thickness of 0.25  $\mu\text{m}$ . The GC oven temperature was maintained at 50°C for 1 min, raised at a rate of 10°C/min to 60°C (held for 2 min), and then further raised at a rate of 10°C/min to 250°C (held for 5 min). The MS ion source temperature was 300°C and the electron energy was 70 eV. Identification of the compounds was based on the NIST 05 mass spectral library database.

## 2. Results and discussion

### 2.1. Optimization of process parameters

#### 2.1.1. Current density

Current density is a primary parameter in contaminant removal and capital cost during electrochemical wastewater treatment (Costa et al., 2009). Therefore, it is crucial to optimize the current density. In order to determine the effect

of the current density on the removal efficiencies of  $\text{COD}_{\text{Cr}}$ ,  $\text{NH}_3\text{-N}$ , TOC, and  $\text{UV}_{254}$  of acrylic fiber wastewater for the 3D-EC reactor, current densities were subsequently set at 120, 310, 500, and 680  $\text{A}/\text{m}^2$  and the other conditions were fixed (circulation rate of 0 mL/min, AC dosage of 50 g, and chloride concentration of 0 g/L).

Fig. 2 shows that the removal efficiencies of  $\text{COD}_{\text{Cr}}$ ,  $\text{NH}_3\text{-N}$ , TOC, and  $\text{UV}_{254}$  were improved with the increase of current density. When the current density was 500  $\text{A}/\text{m}^2$ , the maximum removal efficiencies of  $\text{COD}_{\text{Cr}}$ ,  $\text{NH}_3\text{-N}$ , TOC, and  $\text{UV}_{254}$  in 120 min were 60.5%, 43.0%, 45.2%, and 55.0%, respectively. There was minimal effect on the removal efficiencies of  $\text{COD}_{\text{Cr}}$ ,  $\text{NH}_3\text{-N}$ , TOC, and  $\text{UV}_{254}$  when the current density was increased further. This could be because the oxygen evolution at the anode was enhanced under higher current density (Sirés et al., 2006). Therefore, the optimal current density was 500  $\text{A}/\text{m}^2$ .

#### 2.1.2. Circulation rate

The circulation rate had a great impact on the mass transfer coefficient, which is related to the removal efficiencies of contaminants in electrochemical oxidation (Souza et al., 2014). In the current study, when the circulation rate was set at 0, 5.0, 9.0, and 13.3 mL/min, the effect on the removal efficiencies of  $\text{COD}_{\text{Cr}}$ ,  $\text{NH}_3\text{-N}$ , TOC, and  $\text{UV}_{254}$  was investigated at a current density of 500  $\text{A}/\text{m}^2$ , AC dosage of 50 g, and chloride concentration of 0 g/L.

Fig. 3 indicates that the  $\text{COD}_{\text{cr}}$ ,  $\text{NH}_3\text{-N}$ , TOC, and  $\text{UV}_{254}$  removal rate of the reactor first increased and then decreased with the increase of circulation rate. When the circulation rate was increased from 0 to 5 mL/min, the removal rates of  $\text{COD}_{\text{cr}}$ ,  $\text{NH}_3\text{-N}$ , TOC, and  $\text{UV}_{254}$  were increased from 61.9%, 45.9%, 43.2%, and 53.1% to 68.2%, 55.3%, 57.3%, and 63.5% respectively. However, the  $\text{COD}_{\text{cr}}$ ,  $\text{NH}_3\text{-N}$ , TOC, and  $\text{UV}_{254}$  removal efficiency decreased when the circulation rate was increased further. In comparison to the two-dimensional electrochemical oxidation (2D-EC) reactor, with introduction of AC particle micro-electrodes, the distance between the anode and the cathode of each adjacent bipolar cell was smaller in the 3D-EC reactor, which was conducive to the migration of reagents among the surface of electrodes (Sun et al., 2015b). In addition, an air compressor was used to supply the oxygen essential to the electrochemical reactions in the current study. Wu et al. (2008) reported that the oxygen can be changed into a stronger oxidizing agent,  $\text{H}_2\text{O}_2$ , in the three-phase three-dimensional electrode system. Thus, the 3D-EC reactor could simultaneously make use of anodic oxidation, cathodic electro-generated  $\text{H}_2\text{O}_2$ , and numerous AC micro-electrodes to eliminate the organic pollutants. We also observed that the performance of pollutant mass transfer was improved when the circulation rate was no more than 5 mL/min. However, when the circulation rate was as high as 13.3 mL/min, the disturbance in the oriented flow of the wastewater was detrimental to the migration process among reagents and the surface of electrodes. Moreover, the dissolved oxygen was

taken away from the 3D-EC reactor with the rapid flow. That is why the removal efficiencies of organics decreased with excessive circulation rate. The suitable circulation rate of 5.0 mL/min in the 3D-EC reactor was selected for further optimization studies.

### 2.1.3. AC dosage

AC particles played an important role in the 3D-EC reactor, with the formation of charged micro-electrode particles under the influence of an electric field, which could result in a high degradation efficiency (Kong et al., 2006). The characteristic excellent adsorption capacity of AC allows the pollutants in the wastewater to concentrate on its surface, so that the pollutants could be easily and directly oxidized using the micro-electrodes (Zhu et al., 2011). Therefore, an appropriate AC dosage for the 3D-EC reactor can not only reduce the energy consumption and running cost, but also improve the water quality of the effluent. Therefore, the performance of the 3D-EC reactor was evaluated under various AC dosages: the AC dosage was set at 0, 25, 50, and 60 g and the other conditions were fixed (current density of  $500 \text{ A/m}^2$ , circulation rate of 5 mL/min, and chloride concentration of 0 g/L).

Fig. 4 shows that the removal efficiencies of  $\text{COD}_{\text{cr}}$ ,  $\text{NH}_3\text{-N}$ , TOC, and  $\text{UV}_{254}$  increased when the AC dosage was increased from 0 g to 50 g. The maximum removal efficiencies of  $\text{COD}_{\text{cr}}$ ,  $\text{NH}_3\text{-N}$ , TOC, and  $\text{UV}_{254}$  under the AC dosage of 50 g in 120 min were 69.6%, 56.2%, 58.1%, and 63.8%, respectively. In contrast, the maximum removal efficiencies of  $\text{NH}_3\text{-N}$ , TOC,

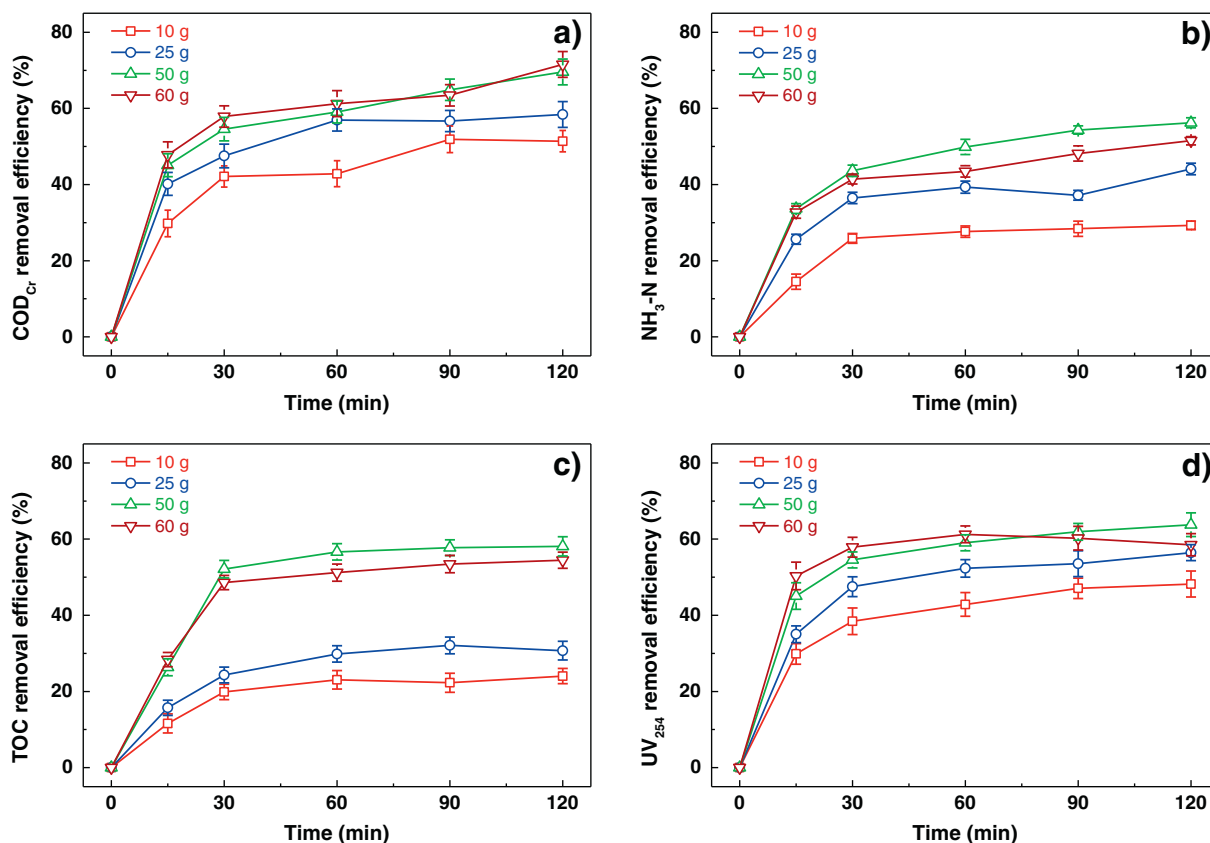


Fig. 4 – The effect of AC dosage on the removal efficiencies of  $\text{COD}_{\text{cr}}$ ,  $\text{NH}_3\text{-N}$ , TOC, and  $\text{UV}_{254}$  for the 3D-EC reactor. Error bars represent standard deviation of three replicates.

and  $UV_{254}$  decreased and the maximum  $COD_{cr}$  removal efficiencies slightly increased under the AC dosage of 60 g for the same reaction time. This could be because the presence of such a large amount of AC particles led to a short circuit, which decreased the removal capacity (Wang et al., 2013). Therefore, the optimal AC dosage for the 3D-EC reactor was 50 g.

#### 2.1.4. Chloride concentration

In general, with the introduction of electrolyte (such as chloride), which is applied to enhance the mass transfer coefficient, the electrochemical oxidation efficacy in the 3D-EC reactor can be improved (Yasri et al., 2015). When the chloride concentration was varied from 0.5 to 2.0 g/L at 0.5 g/L intervals, the effects on the removals of  $COD_{cr}$ ,  $NH_3-N$ , TOC, and  $UV_{254}$  were investigated under conditions of a current density of 500 A/m<sup>2</sup>, circulation rate of 5 mL/min, and AC dosage of 50 g.

Fig. 5 shows that removal efficiencies of  $COD_{cr}$ ,  $NH_3-N$ , TOC, and  $UV_{254}$  at 120 min mostly first increased and then decreased with the increase of chloride concentration, and reached a peak for the chloride concentration of 1.0 g/L. The removal efficiencies of  $COD_{cr}$ ,  $NH_3-N$ , TOC, and  $UV_{254}$  at 120 min were 74.8%, 72.1%, 57.5%, and 79.0% respectively under the above described conditions. With the exception of a somewhat complex variation of  $UV_{254}$  under different chloride concentrations, the removal efficiencies of  $COD_{cr}$ ,  $NH_3-N$ , and

TOC maintained the same decreasing pace when the chloride concentration continuously increased beyond the concentration of 1.0 g/L. Indeed, the degradation process could be improved by active chlorine, which was generated with the addition of chloride ions during the 3D-EC process. This did not mean that the improvement was infinite (Dai et al., 2013). Thus, the optimal chloride concentration for the 3D-EC reactor was 1.0 g/L.

In addition, compared with the maximum removal efficiencies of contaminants under the optimized conditions in Section 2.1.3 (current density of 500 A/m<sup>2</sup>, circulation rate of 5 mL/min, AC dosage of 50 g, and chloride concentration of 0 g/L), the maximum removal efficiencies of  $COD_{cr}$ ,  $NH_3-N$ , TOC, and  $UV_{254}$  at 120 min under the optimal chloride concentration of 1.0 g/L increased 7.5%, 28.3%, -1.0%, and 23.8%. Interestingly, with the addition of chloride electrolyte, the  $NH_3-N$  removal increment was much higher than that of  $COD_{cr}$ . This could be explained by the competition between  $NH_3-N$  and  $COD_{cr}$  removal by indirect oxidation, via chlorine/hypochlorite species in the system, and consequently the  $NH_3-N$  removal rate became much higher than that of  $COD_{cr}$ . This result was also observed in previous studies (Chiang et al., 1995; Zhang et al., 2010, 2011). In addition, the ammonia was eliminated through the formation of equal molar amounts of nitrogen gas and nitrous oxide. A similar phenomenon was also found in a previous study (Pérez et al., 2012).

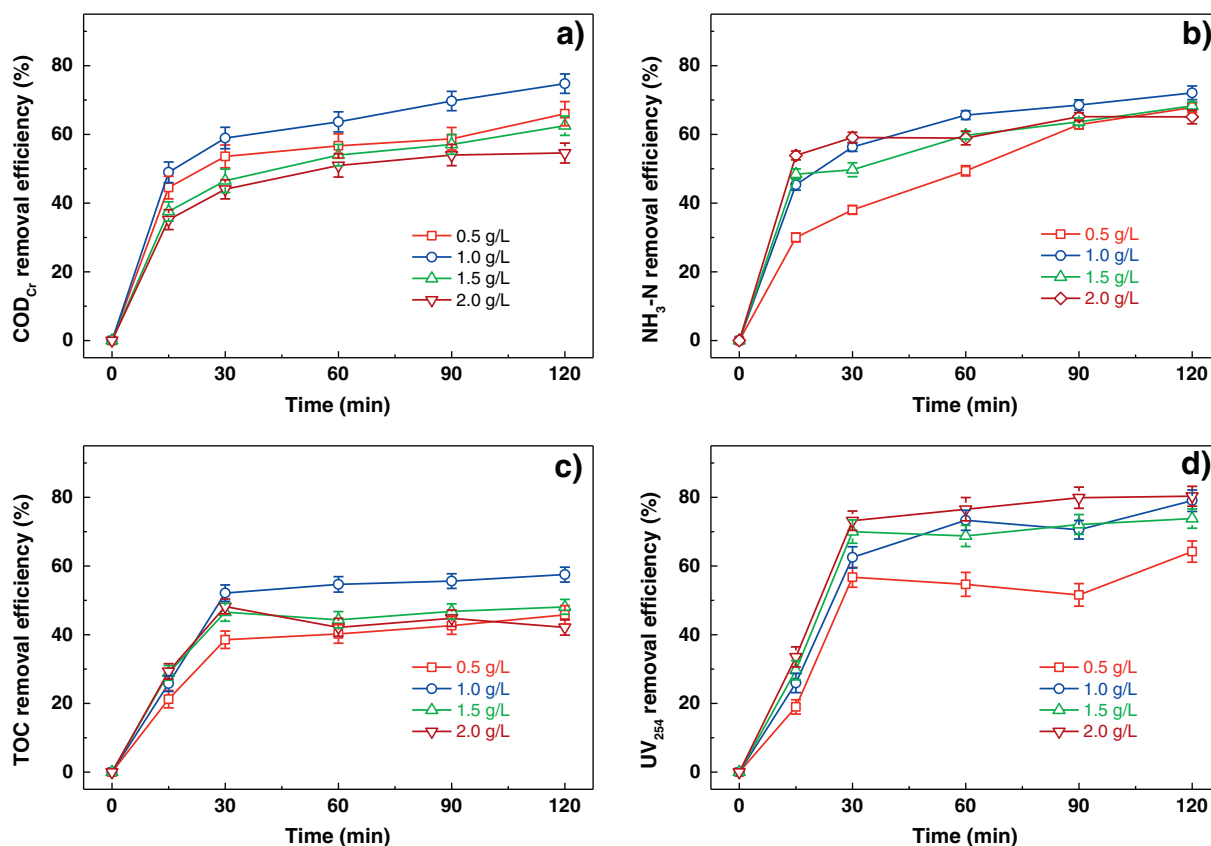


Fig. 5 – The effect of chloride concentration on the removal efficiencies of  $COD_{cr}$ ,  $NH_3-N$ , TOC, and  $UV_{254}$  for the 3D-EC reactor. Error bars represent standard deviation of three replicates.

2.1.5. Overall performance under the optimized conditions

In conclusion, the optimized operational parameters in the 3D-EC reactor were a current density of 500 A/m<sup>2</sup>, circulation rate of 5 mL/min, AC dosage of 50 g, and chloride concentration of 1.0 g/L. Without replacing the AC particles in the 3D-EC system, 20 repeated trials were carried out and the removals of contaminants in terms of COD<sub>cr</sub>, NH<sub>3</sub>-N, TOC, and UV<sub>254</sub> were determined (Fig. 6).

Fig. 6 shows that the average removal efficiencies of COD<sub>cr</sub>, NH<sub>3</sub>-N, TOC, and UV<sub>254</sub> were 64.5% ± 4.6%, 60.8% ± 3.5%, 46.4% ± 3.3%, and 64.8% ± 3.6% respectively, while the influent concentrations of COD<sub>cr</sub>, NH<sub>3</sub>-N, TOC, and UV<sub>254</sub> were 215.8 ± 10.3, 51.2 ± 4.8, and 79.3 ± 13.4 mg/L, and 0.23 ± 0.02 Abs/cm. The wastewater contaminants were eliminated by the 3D-EC reactor: the effluent concentrations of COD<sub>cr</sub>, NH<sub>3</sub>-N, TOC, and UV<sub>254</sub> were 76.6 ± 11.0, 20.1 ± 2.8, and 42.5 ± 7.7 mg/L, and 0.08 ± 0.01 Abs/cm accordingly. The effluent concentration of COD<sub>cr</sub> was less than 100 mg/L, which meant that the treated wastewater reached the integrated wastewater discharge standard (GB 8978-1996).

2.2. Synergistic effect of the 3D-EC reactor

The removal efficiencies of COD<sub>cr</sub>, NH<sub>3</sub>-N, TOC, and UV<sub>254</sub> in the 3D-EC process and separated processes (i.e., 2D-EC alone and AC adsorption alone, the other parameters were consistent) are shown in Fig. 7.

Fig. 7 shows that the repeated trials were obviously divided into two stages according to the run number. Combined with the evaluation of the removal efficiencies of contaminants (Fig. 6), the start-up stage was defined as when the run number was no more than 5 and the stable stage was defined as when the run number ranged from 5 to 20. Under the stable stage, the 2D-EC process alone only reduced 7.5% ± 0.3% COD<sub>cr</sub>, 16.2% ± 0.4% NH<sub>3</sub>-N, 13.3% ± 1.1% TOC, and 25.0% ± 1.5% UV<sub>254</sub>. The AC adsorption alone showed better removal rates for COD<sub>cr</sub>, NH<sub>3</sub>-N, TOC, and UV<sub>254</sub> (i.e., 35.9% ± 2.7%, 26.6% ± 1.1%, 22.2% ± 1.2%, and 32.4% ± 2.1%, respectively), which could be ascribed to the greater adsorption capacity of the AC particles.

The 3D-EC process removed COD<sub>cr</sub> by 62.7% ± 1.9%, NH<sub>3</sub>-N by 59.4% ± 0.7%, TOC by 45.1% ± 1.3%, and UV<sub>254</sub> by 62.7% ± 1.9%, which was much higher than the sum of the individual removal rates of the two separated processes.

The synergistic efficiency (η) of the 3D-EC process could be calculated by Eq. (1)

$$\eta = \frac{R_{3D-EC} - (R_{2D-EC} + R_{AC})}{R_{2D-EC} + R_{AC}} \times 100\% \tag{1}$$

where R<sub>3D-EC</sub>, R<sub>2D-EC</sub>, and R<sub>AC</sub> represent the removal rates in 2D-EC process alone, AC adsorption alone, and the 3D-EC process, respectively. As calculated in Eq. (1), the synergistic efficiencies (η) in COD<sub>cr</sub>, NH<sub>3</sub>-N, TOC, and UV<sub>254</sub> removal are shown in Table 2.

Table 2 indicates that the 3D-EC process has excellent performance, with the synergistic efficiencies of COD<sub>cr</sub>, NH<sub>3</sub>-N,

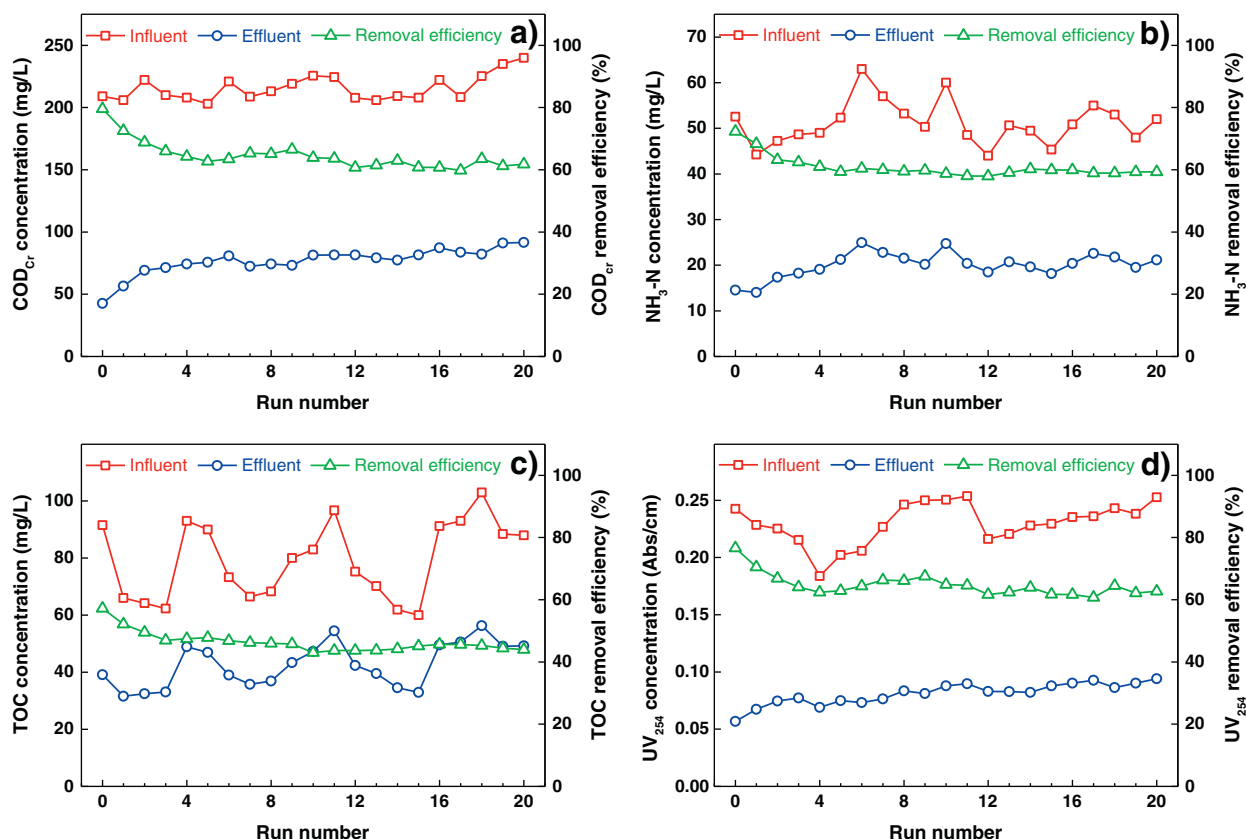


Fig. 6 – The removal of contaminants in the 3D-EC reactor under the optimized condition.

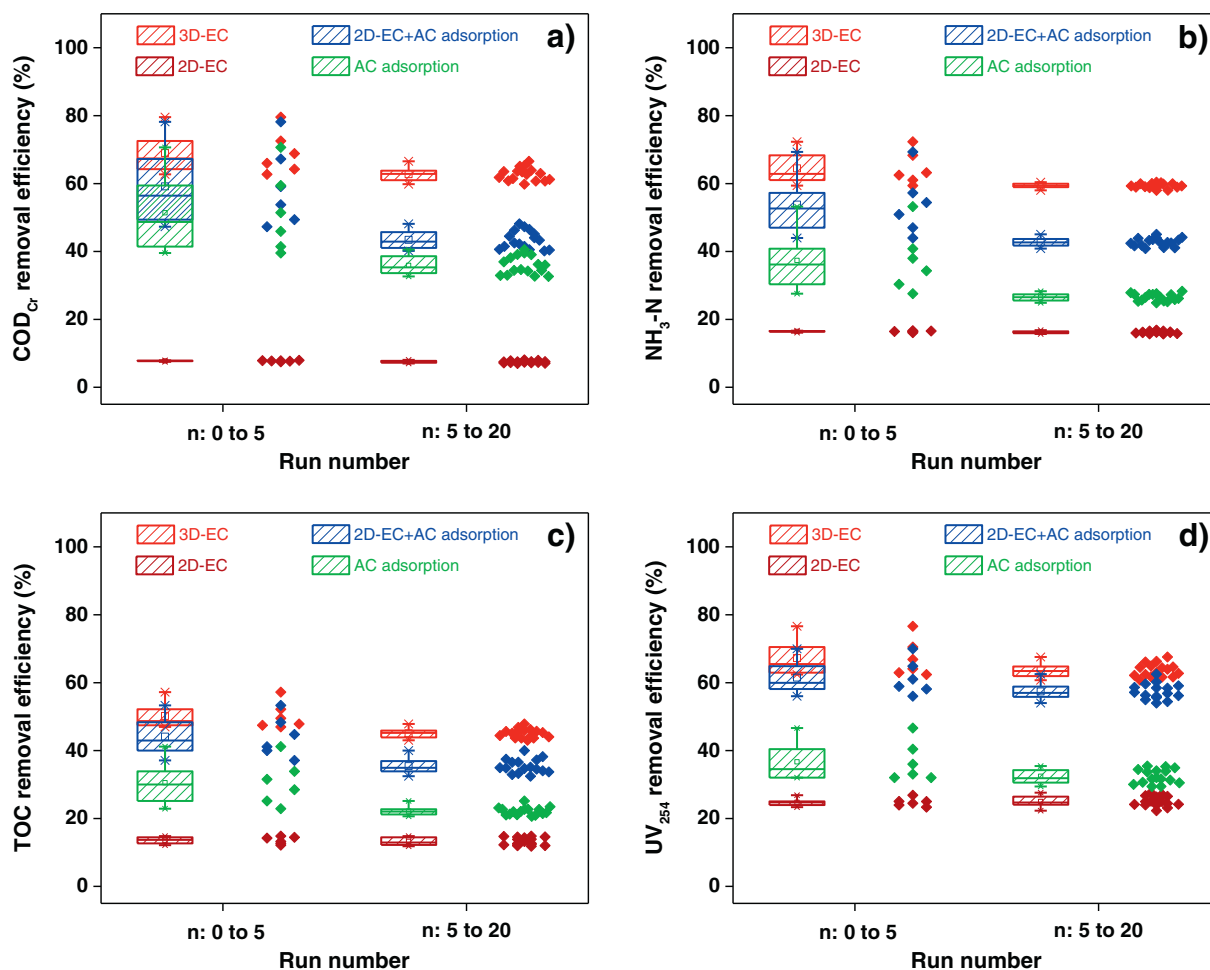


Fig. 7 – The removal efficiencies of  $\text{COD}_{\text{Cr}}$ ,  $\text{NH}_3\text{-N}$ , TOC, and  $\text{UV}_{254}$  in the 3D-EC process and the separated processes.

TOC, and  $\text{UV}_{254}$  in the start-up stage being 16.6%, 19.8%, 13.8%, and 9.3%, respectively. Compared with the start-up stage, the synergistic efficiencies in the stable stage were further strengthened, with the synergistic efficiencies of  $\text{COD}_{\text{Cr}}$ ,  $\text{NH}_3\text{-N}$ , TOC, and  $\text{UV}_{254}$  as high as 44.5%, 38.8%, 27.2%, and 10.9%. With regard to the approximate removal efficiencies of contaminants in the start-up and stable stages during the 2D-EC process alone, the difference in the synergistic efficiencies in the two processes was primarily caused by the AC adsorption. It is easy to understand that the AC adsorption capacity was not fully saturated at the first 5 repeated trials; and then its capacity

was stable during the operation of 3D-EC reactor, which also could be explained using the standard deviation of the removal efficiencies of  $\text{COD}_{\text{Cr}}$ ,  $\text{NH}_3\text{-N}$ , TOC, and  $\text{UV}_{254}$  in the two stages during the AC adsorption alone process (Table 2). Therefore, a significant improvement in contaminant degradation was achieved in the 3D-EC process.

### 2.3. Enhancement in the degradation of organics

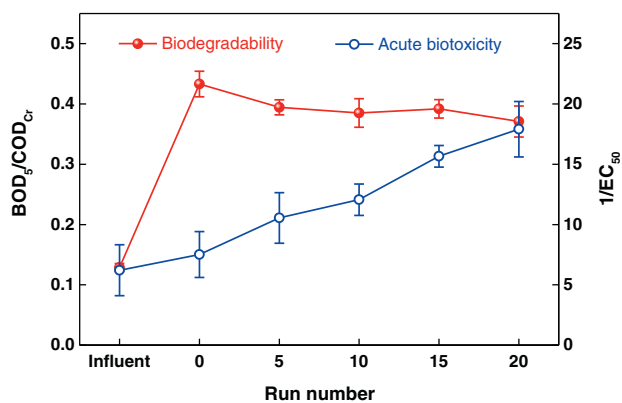
Fig. 8 shows that the calculated  $\text{BOD}_5/\text{COD}_{\text{Cr}}$  ratio increased from  $0.13 \pm 0.01$  to  $0.43 \pm 0.02$  in the 3D-EC reactor, and then

Table 2 – Variation of  $\text{COD}_{\text{Cr}}$ ,  $\text{NH}_3\text{-N}$ , TOC and  $\text{UV}_{254}$  removal in 2D-EC process alone, AC adsorption alone, and 3D-EC process.

Items	Removal efficiency (%) in start-up stage (n: 0 to 5)				Removal efficiency (%) in stable stage (n: 5 to 20)			
	$\text{COD}_{\text{Cr}}$	$\text{NH}_3\text{-N}$	TOC	$\text{UV}_{254}$	$\text{COD}_{\text{Cr}}$	$\text{NH}_3\text{-N}$	TOC	$\text{UV}_{254}$
2D-EC process alone	$7.8 \pm 0.2$	$16.4 \pm 0.2$	$13.6 \pm 1.1$	$24.8 \pm 1.2$	$7.5 \pm 0.3$	$16.2 \pm 0.4$	$13.2 \pm 1.1$	$25.0 \pm 1.5$
AC adsorption alone	$51.4 \pm 11.9$	$37.4 \pm 9.1$	$30.5 \pm 6.6$	$36.7 \pm 5.8$	$35.9 \pm 2.7$	$26.5 \pm 1.1$	$22.2 \pm 1.2$	$32.4 \pm 2.1$
3D-EC process	$69.0 \pm 6.3$	$64.5 \pm 4.9$	$50.2 \pm 3.9$	$67.2 \pm 5.5$	$62.7 \pm 1.9$	$59.4 \pm 0.7$	$45.1 \pm 1.3$	$63.7 \pm 2.0$
Synergistic efficiency calculated (%)	16.6	19.8	13.8	9.3	44.5	38.8	27.2	10.9

$\text{COD}_{\text{Cr}}$ : chemical oxygen demand; TOC: total organic carbon;  $\text{UV}_{254}$ : ultraviolet absorption at 254 nm; 2D-EC: two-dimensional electrochemical oxidation; AC: activated carbon; 3D-EC: three-dimensional electrochemical oxidation.





**Fig. 8 – The variation of biodegradability and acute biotoxicity.**

slightly decreased with the increase of run number, demonstrating decreased biodegradability. At the same time, the acute biotoxicity in wastewater continued to increase during the repeated trials. The variation of biodegradability and acute biotoxicity in wastewater may be caused by the formation of more toxic organics and oxidants in the 3D-EC reactor (Wang et al., 2014). Therefore, the electrochemical process should be carefully evaluated during the advanced oxidation treatment of wastewater, because the increase in acute biotoxicity might result in high environmental risks when the treated wastewater is directly discharged into receiving water.

GC-MS analysis was applied to identify the organic compounds in the raw and treated wastewater. The chromatograms are shown in Fig. 9 and the variations of chemicals are summarized in Table 3. These compounds

include 12 kinds of alkanes (accounting for 91.6% total peak area, and interestingly “heneicosane” appeared three times under the retention times of 18.375, 22.383, and 25.175 min), 5 aromatic compounds (accounting for 3.9% total peak area), and 4 esters (accounting for 3.0% total peak area). A small number of phenols (2, 1%), an organic nitrile (1, 0.5%), and an amide (1, 0.1%) were also identified. Among these long-chain alkane compounds, the carbon numbers of alkanes (except decane) varied from 15 to 40, which are bio-refractory in the conventional biological treatment (Tong et al., 2013). Both aromatic compounds and organic nitriles are toxic and refractory. This result may explain why the biodegradability of the raw wastewater (shown in Table 1) was very low.

By comparison to Fig. 9a, the chromatograph of Fig. 9b shows that most organic pollutants were significantly removed after the 3D-EC treatment. The compounds remaining in the effluent were long-chain alkanes; nevertheless, more than 86.6% of major alkanes was eliminated. Based on the overall performance, it can be concluded that organic compounds with higher molecular weight were converted into smaller molecules with more favorable biodegradable characteristics, which revealed that there was no other toxic organic generation during the electrochemical treatment. Thus, the generation of oxidants such as active chlorine ( $\text{Cl}_2$ ,  $\text{ClO}^-$ , and  $\text{HClO}$ ) may be responsible for the acute biotoxicity increase after the treatment.

During the repeated trials, with the increase in introduced chloride electrolyte, the formation of free chlorine might be centralized in the 3D-EC reactor. In order to investigate whether free chlorine was responsible for the increase in biotoxicity, a certain concentration of  $\text{Na}_2\text{SO}_3$  was applied to eliminate the interference of free chlorine. The results showed that the acute biotoxicity declined to zero, indicating that the generation of acute biotoxicity is caused by free chlorine generated in the 3D-EC reactor. A similar result was

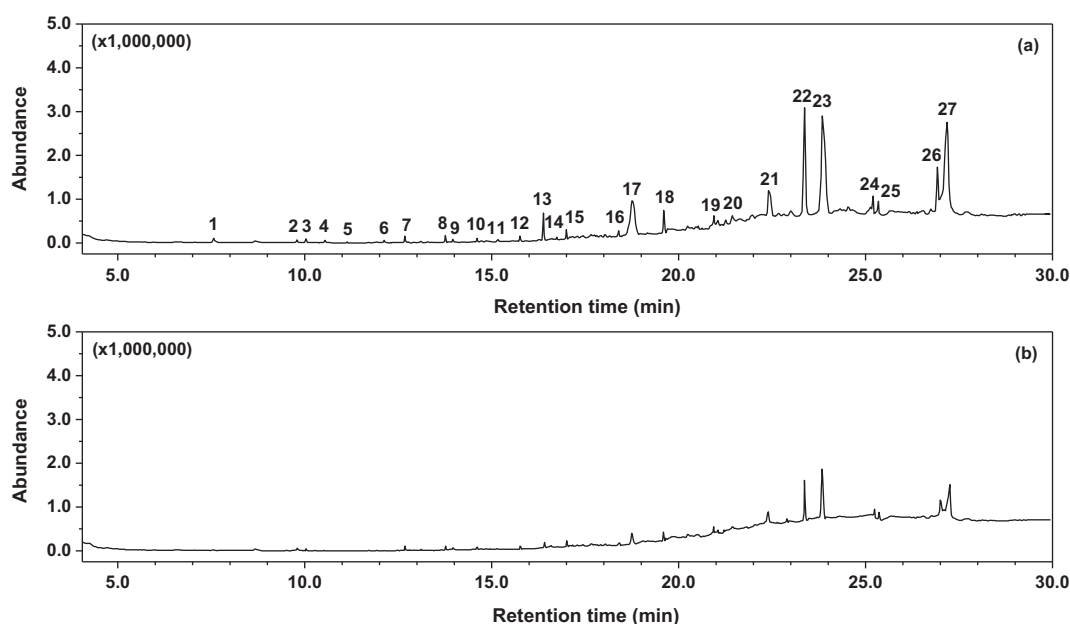


**Fig. 9 – GC-MS chromatograms of (a) raw wastewater, (b) wastewater treated by the 3D-EC process.**

**Table 3 – The main organic pollutants identified in the raw and treated wastewater with GC–MS.**

No.	Retention time (min)	Chemicals	Similarity (%)	Area (mean ± S.D.)	Removal efficiency (%) (mean ± S.D.)
1	7.492	Toluene	92	13574 ± 1829	96.2 ± 0.5
2	9.783	Ethyl-benzene	90	8457 ± 1176	67.7 ± 0.7
3	10.000	1,2-Dimethyl-benzene	88	7937 ± 2205	79.1 ± 1.2
4	10.508	Ethenyl-benzene	90	5832 ± 1109	92.4 ± 2.1
5	11.142	N,N-dimethylacetamide	81	1591 ± 276	88.1 ± 1.3
6	12.083	Benzenol	93	5012 ± 1002	92.3 ± 0.8
7	12.642	Decane	95	25987 ± 453	65.1 ± 1.4
8	13.742	Sulfuric acid, hexyl octyl ester	86	15955 ± 700	61.9 ± 2.0
9	13.950	2-Methyleneglutaronitrile	92	6709 ± 333	75.7 ± 1.4
10	14.592	4,6-Dimethyl-dodecane	89	11354 ± 238	73.2 ± 2.4
11	15.133	Pentanedioic acid, dimethyl ester	89	6594 ± 230	85.5 ± 2.6
12	15.733	2-Phenyl-tridecane	84	20491 ± 2209	70.4 ± 1.7
13	16.367	Pentadecane	96	112163 ± 2870	97.2 ± 1.8
14	16.742	Oxalic acid, 4-chlorophenyl octyl ester	82	3703 ± 761	94.9 ± 1.6
15	16.983	Adipic acid, ethyl methyl ester	85	16969 ± 595	72.3 ± 2.0
16	18.375	Heneicosane	96	15270 ± 557	79.8 ± 2.4
17	18.717	Heptadecane	96	102989 ± 2522	96.9 ± 1.4
18	19.567	Hexadecane	96	89171 ± 1916	92.7 ± 2.4
19	20.900	Eicosane	97	31954 ± 839	76.1 ± 0.9
20	21.242	2,4-Di-tert-butylphenol	91	8819 ± 1491	85.8 ± 1.2
21	22.383	Heneicosane	91	34015 ± 1005	87.5 ± 2.5
22	23.333	Pentacosane	92	285396 ± 11649	89.3 ± 2.2
23	23.800	Dotriacontane	88	242974 ± 9047	81.7 ± 1.6
24	25.175	Heneicosane	92	59007 ± 1844	78.0 ± 2.8
25	25.300	Tetracosane	92	43183 ± 1623	75.9 ± 1.3
26	26.925	Hexatriacontane	93	61068 ± 2205	92.7 ± 1.5
27	27.117	Tetracontane	91	210318 ± 11069	88.8 ± 1.2

GC–MS: gas chromatography mass spectrometry; S.D.: standard deviation.

also derived by Wang et al. (2014), who reported that the acute biotoxicity was greatly increased (more than 95% inhibition) by the generation of free chlorine. Therefore, the 3D-EC process is an effective technique for the treatment of secondary wet-spun acrylic fiber manufacturing wastewater.

### 3. Conclusions

The 3D-EC process is a promising advanced oxidation process that can be applied for the treatment of refractory wet-spun acrylic fiber manufacturing wastewater. When the influent concentrations of COD<sub>cr</sub>, NH<sub>3</sub>-N, TOC, and UV<sub>254</sub> were 215.8 ± 10.3, 51.2 ± 4.8, and 79.3 ± 13.4 mg/L, and 0.23 ± 0.02 Abs/cm respectively, 64.5% ± 4.6% of COD<sub>cr</sub>, 60.8% ± 3.5% of NH<sub>3</sub>-N, 46.4% ± 3.3% of TOC, and 64.8% ± 3.6% of UV<sub>254</sub> could be removed by the 3D-EC reactor under optimized conditions (current density of 500 A/m<sup>2</sup>, circulation rate of 5 mL/min, AC dosage of 50 g, and chloride concentration of 1.0 g/L). Further, a significant synergetic effect existed between the 2D-EC and AC adsorption processes for the removals of COD<sub>cr</sub>, NH<sub>3</sub>-N, TOC, and UV<sub>254</sub> during the stable stage, which was ascribed to numerous AC micro-electrodes in the 3D-EC reactor. The biodegradability (BOD<sub>5</sub>/COD<sub>cr</sub>) of the 3D-EC reactor was initially improved from 0.13 to 0.43, and then slightly decreased with the increase of repeated runs; however, the acute biotoxicity of the wastewater continuously increased at the same time. Based on the analysis with GC–MS, there were no toxic organics

generated by the electrochemical treatment. Further, the increase of acute biotoxicity was mainly attributed to the production of free chlorine.

### Acknowledgments

This work was supported by the Major Science and Technology Program for Water Pollution Control and Treatment (No. 2012ZX07201002-6). Thanks are also extended to China Oil HBP Science & Technology Co., Ltd. for providing the wastewater.

### REFERENCES

- An, P., Xu, X., Yang, F., Liu, L., Liu, S., 2013. A pilot-scale study on nitrogen removal from dry-spun acrylic fiber wastewater using anammox process. *Chem. Eng. J.* 222, 32–40.
- Anglada, A., Urriaga, A., Ortiz, I., 2009. Pilot scale performance of the electro-oxidation of landfill leachate at boron-doped diamond anodes. *Environ. Sci. Technol.* 43 (6), 2035–2040.
- Chiang, L.C., Chang, J.E., Wen, T.C., 1995. Indirect oxidation effect in electrochemical oxidation treatment of landfill leachate. *Water Res.* 29 (2), 671–678.
- Costa, C.R., Montilla, F., Morallón, E., Olivi, P., 2009. Electrochemical oxidation of acid black 210 dye on the boron-doped diamond electrode in the presence of phosphate ions: effect of current density, pH, and chloride ions. *Electrochim. Acta* 54 (27), 7048–7055.

- Dai, Q., Shen, H., Xia, Y., Chen, F., Wang, J., Chen, J., 2013. The application of a novel Ti/SnO<sub>2</sub>-Sb<sub>2</sub>O<sub>3</sub>/PTFE-La-Ce-β-PbO<sub>2</sub> anode on the degradation of cationic gold yellow X-GL in sono-electrochemical oxidation system. *Sep. Purif. Technol.* 104, 9–16.
- Fernandes, A., Santos, D., Pacheco, M.J., Ciriaco, L., Lopes, A., 2016. Electrochemical oxidation of humic acid and sanitary landfill leachate: influence of anode material, chloride concentration and current density. *Sci. Total Environ.* 541, 282–291.
- Gong, C., Zhang, Z., Li, H., Li, D., Wu, B., Sun, Y., et al., 2014. Electrocoagulation pretreatment of wet-spun acrylic fibers manufacturing wastewater to improve its biodegradability. *J. Hazard. Mater.* 274, 465–472.
- Kong, W., Wang, B., Ma, H., Gu, L., 2006. Electrochemical treatment of anionic surfactants in synthetic wastewater with three-dimensional electrodes. *J. Hazard. Mater.* 137 (3), 1532–1537.
- Lai, B., Zhou, Y., Qin, H., Wu, C., Pang, C., Lian, Y., Xu, J., 2012. Pretreatment of wastewater from acrylonitrile-butadiene-styrene (ABS) resin manufacturing by microelectrolysis. *Chem. Eng. J.* 179, 1–7.
- Li, J., Wang, J., Luan, Z., Deng, Y., Chen, L., 2011. Evaluation of performance and microbial community in a two-stage UASB reactor pretreating acrylic fiber manufacturing wastewater. *Bioresour. Technol.* 102 (10), 5709–5716.
- Li, J., Wang, J., Luan, Z., Ji, Z., Yu, L., 2012. Biological sulfate removal from acrylic fiber manufacturing wastewater using a two-stage UASB reactor. *J. Environ. Sci.* 24 (2), 343–350.
- Li, J., Yu, D., Zhang, P., 2013. Partial nitrification in a sequencing batch reactor treating acrylic fiber wastewater. *Biodegradation* 24 (3), 427–435.
- Martins, R.C., Rossi, A.F., Quinta-Ferreira, R.M., 2010. Fenton's oxidation process for phenolic wastewater remediation and biodegradability enhancement. *J. Hazard. Mater.* 180 (1–3), 716–721.
- Pérez, G., Saiz, J., Ibañez, R., Urriaga, A.M., Ortiz, I., 2012. Assessment of the formation of inorganic oxidation by-products during the electrocatalytic treatment of ammonium from landfill leachates. *Water Res.* 46 (8), 2579–2590.
- Sirés, I., Cabot, P.L., Centellas, F., Garrido, J.A., Rodríguez, R.M., Arias, C., Brillas, E., 2006. Electrochemical degradation of clofibric acid in water by anodic oxidation: comparative study with platinum and boron-doped diamond electrodes. *Electrochim. Acta* 52 (1), 75–85.
- Souza, F.L., Aquino, J.M., Miwa, D.W., Rodrigo, M.A., Motheo, A.J., 2014. Electrochemical degradation of dimethyl phthalate ester on a DSA® electrode. *J. Braz. Chem. Soc.* 25 (3), 492–501.
- Sun, M., Chen, F., Qu, J., Liu, H., Liu, R., 2015a. Optimization and control of Electro-Fenton process by pH inflection points: a case of treating acrylic fiber manufacturing wastewater. *Chem. Eng. J.* 269, 399–407.
- Sun, H., Chen, T., Kong, L., Cai, Q., Xiong, Y., Tian, S., 2015b. Potential of sludge carbon as new granular electrodes for degradation of acid orange 7. *Ind. Eng. Chem. Res.* 54 (20), 5468–5474.
- Tian, Z., Xin, W., Song, Y., Li, F., 2015. Simultaneous organic carbon and nitrogen removal from refractory petrochemical dry-spun acrylic fiber wastewater by hybrid A/O-MBR process. *Environ. Earth Sci.* 73 (9), 4903–4910.
- Tong, K., Zhang, Y., Liu, G., Ye, Z., Chu, P.K., 2013. Treatment of heavy oil wastewater by a conventional activated sludge process coupled with an immobilized biological filter. *Int. Biodeter. Biodegr.* 84, 65–71.
- Urriaga, A., Fernandez-Castro, P., Gómez, P., Ortiz, I., 2014. Remediation of wastewaters containing tetrahydrofuran. Study of the electrochemical mineralization on BDD electrodes. *Chem. Eng. J.* 239, 341–350.
- Wang, A.M., Qu, J.H., Liu, H.J., Lei, P.J., 2005. Dyes wastewater treatment by reduction-oxidation process in an electrochemical reactor packed with natural manganese mineral. *J. Environ. Sci. (China)* 18 (1), 17–22.
- Wang, B., Kong, W., Ma, H., 2007. Electrochemical treatment of paper mill wastewater using three-dimensional electrodes with Ti/Co/SnO<sub>2</sub>-Sb<sub>2</sub>O<sub>3</sub> anode. *J. Hazard. Mater.* 146 (1), 295–301.
- Wang, L., Hu, Y., Li, P., Zhang, Y., Yan, Q., Zhao, Y., 2013. Electrochemical treatment of industrial wastewater using a novel layer-upon-layer bipolar electrode system (nLBPEs). *Chem. Eng. J.* 215–216, 157–161.
- Wang, C., Huang, Y., Zhao, Q., Ji, M., 2014. Treatment of secondary effluent using a three-dimensional electrode system: COD removal, biotoxicity assessment, and disinfection effects. *Chem. Eng. J.* 243, 1–6.
- Wei, F.S., Qi, W.Q., Sun, Z.G., Huang, Y.R., Shen, Y.W., 2002. Water and Wastewater Monitoring and Analysis Method. China Environmental Science Press, Beijing.
- Wei, L., Guo, S., Yan, G., Chen, C., Jiang, X., 2010. Electrochemical pretreatment of heavy oil refinery wastewater using a three-dimensional electrode reactor. *Electrochim. Acta* 55 (28), 8615–8620.
- Wu, X., Yang, X., Wu, D., Fu, R., 2008. Feasibility study of using carbon aerogel as particle electrodes for decoloration of RBRX dye solution in a three-dimensional electrode reactor. *Chem. Eng. J.* 138 (1), 47–54.
- Xu, L., Zhao, H., Shi, S., Zhang, G., Ni, J., 2008. Electrolytic treatment of CI Acid Orange 7 in aqueous solution using a three-dimensional electrode reactor. *Dyes Pigments* 77 (1), 158–164.
- Yasri, N.G., Yaghmour, A., Gunasekaran, S., 2015. Effective removal of organics from corn wet milling steepwater effluent by electrochemical oxidation and adsorption on 3-D granulated graphite electrode. *J. Environ. Chem. Eng.* 3 (2), 930–937.
- Zhang, H., Li, Y., Wu, X., Zhang, Y., Zhang, D., 2010. Application of response surface methodology to the treatment landfill leachate in a three-dimensional electrochemical reactor. *Waste Manag.* 30 (11), 2096–2102.
- Zhang, H., Ran, X., Wu, X., Zhang, D., 2011. Evaluation of electro-oxidation of biologically treated landfill leachate using response surface methodology. *J. Hazard. Mater.* 188 (1–3), 261–268.
- Zhang, C., Jiang, Y., Li, Y., Hu, Z., Zhou, L., Zhou, M., 2013. Three-dimensional electrochemical process for wastewater treatment: a general review. *Chem. Eng. J.* 228, 455–467.
- Zheng, T., Wang, Q., Zhang, T., Shi, Z., Tian, Y., Shi, S., Smale, N., Wang, J., 2015a. Microbubble enhanced ozonation process for advanced treatment of wastewater produced in acrylic fiber manufacturing industry. *J. Hazard. Mater.* 287, 412–420.
- Zheng, T., Zhang, T., Wang, Q., Tian, Y., Shi, Z., Smale, N., Xu, B., 2015b. Advanced treatment of acrylic fiber manufacturing wastewater with a combined microbubble-ozonation/ultraviolet irradiation process. *RSC Adv.* 5 (95), 77601–77609.
- Zhu, X., Ni, J., Xing, X., Li, H., Jiang, Y., 2011. Synergies between electrochemical oxidation and activated carbon adsorption in three-dimensional boron-doped diamond anode system. *Electrochim. Acta* 56 (3), 1270–1274.